Contrib Mineral Petrol (1999) 135: 340–354

Anthi Liati · Dieter Gebauer

Constraining the prograde and retrograde *P-T-t* path of Eocene H*P* rocks by SHRIMP dating of different zircon domains: inferred rates of heating, burial, cooling and exhumation for central Rhodope, northern Greece

Received: 5 October 1998 / Accepted: 18 January 1999

Abstract Ion microprobe (SHRIMP) dating was carried out on different zircon domains from metamorphic rocks of the H*P*-H*T* terrane of central Rhodope, northern Greece, to constrain the timing of prograde and retrograde stages within a single tectono-metamorphic cycle. A well determined *P-T-t*(relative) path for the metamorphic rocks of this terrane was used as a petrological basis for the geochronological investigations. Ion microprobe work was assisted by cathodoluminescence (CL) images of the zircon crystals. The geochronological results revealed that Hercynian continental crust was subducted during the Eocene. Several stages of the Eocene tectono-metamorphic cycle – including both the prograde and retrograde parts of the *P-T* path above ca 300 °C, 0.3 GPa – were dated using zircons from the following rock types: (1) A deformed quartz vein probably formed at ca 300 °C, 0.3 GPa. Zircons in this vein precipitated from a hydrothermal fluid; they yielded an age of 45.3 ± 0.9 Ma which corresponds to the time of a low-*T* prograde stage of metamorphism. (2) In kyanite eclogites, zircons were entirely reset during eclogite-facies metamorphism. Resetting was very probably enhanced by the presence of fluids derived by H_2O liberating reactions close to the *P*-peak. They yielded an age of 42.2 ± 0.9 Ma. (3) Orthogneisses surrounding the kyanite eclogites contained zircons with magmatic oscillatory zoned cores, which yielded Hercynian ages of 294 ± 8 Ma (age of granitic protolith formation), whereas CL-bright, metamorphic rims yielded, like the eclogite zircons, ages of 42.0 ± 1.1 Ma. Therefore, both the eclogites and orthogneisses are interpreted to have approached maximum depth at around 42 Ma. (4) In a leucosome of a migmatized orthogneiss, oscillatory zoned zircons yielded an age of 40.0 ± 1.0 Ma. At this time the rocks reached maximum temperatures during early decompression. (5) A late pegmatite crosscutting the schistosity of amphibolites contained oscillatory zoned zircons that yielded a crystallization age of 36.1 ± 1.2 Ma. Thus, the whole tectono-metamorphic cycle above ca 300 °C, 0.3 GPa lasted from 45.3 ± 0.9 Ma to 36.1 ± 1.2 Ma, that is 9.2 Ma with an extreme error value of 2.1 Ma. Based on combined SHRIMP and petrological data, the average rates of heating and burial during subduction (above ca 300 °C, 0.3 GPa) are > 94 °C/Ma and > 15 mm/a, respectively. Rates of cooling and exhumation (also above 300 °C, 0.3 GPa) are calculated to be > 128° C/Ma and > 7.7 mm/a. The Eocene age of metamorphism in central Rhodope implies that the terrane of, at least, central Rhodope and the Cyclades very probably was part of the same continental crust.

A. Liati (✉) · D. Gebauer
Institut für Isotopengeochemie und Mineralische Rohstoffe, ETH-Zentrum, Sonneggstrasse 5, CH-8092, Zürich, Switzerland
E-mail: liati@erdw.ethz.ch

Editorial responsibility: W. Schreyer

Introduction

Constraining the pressure-temperature-time (*P-T-t*) path of a metamorphic terrane is very important for geodynamic interpretations. This is especially true for H*P* terranes where the prograde and retrograde history are relevant to understanding the processes of subduction to great depths and the subsequent exhumation (i.e., burial and exhumation rates, heating and cooling rates, heat and mass transfer). Construction of *P-T-t* paths is commonly based on the relative time of the metamorphic episodes that have affected a certain geological unit. Determination of the absolute time of the metamorphic stages is, however, much more relevant since this allows us to infer the absolute rates of tectono-metamorphic processes. Rates of mass and heat transfer can then be deduced. Such calculations have already been performed so far in several geological units worldwide but generally refer only to a part of the metamorphic evolution, namely the post-peak exhumation history of the rocks.

In an attempt to date low-*T* prograde metamorphism, in addition to other stages, within a single tectono-

metamorphic cycle, we selected the H*P*-H*T* terrane of Rhodope, northern Greece. Here, a well constrained and quite precisely determined P-T-$t_{(rel)}$ path has been proposed by Liati and Seidel (1996), which can be used as a petrological basis for the geochronological investigations. In order to date the prograde metamorphic stage at low temperatures, we separated hydrothermally formed zircons from a synmetamorphic, deformed quartz vein intercalated within paragneisses. Quartz veins of this type form at the early stages of subduction, during incipient metamorphism and associated fluid liberation as the result of dehydration reactions (e.g., Manning 1996; Jamtveit and Yardley 1997; Yardley 1997). To date the peak of metamorphism, we used zircons from two kyanite eclogites and one surrounding orthogneiss, as well as from a leucosome of a migmatized orthogneiss. For the late, low-T, retrograde stage of the P-T-t path, we dated an undeformed pegmatite crosscutting the schistosity of the metamorphic rocks. Based on the obtained ages, we calculated heating and cooling rates, as well as burial and exhumation rates from the early stages of subduction (ca 300 °C, 0.3 GPa), through the peak of metamorphism to late exhumation stages (ca 300 °C, 0.3 GPa).

Because of the complicated formation history of the rocks, zircon crystals usually show complex growth patterns and crystal shapes in cathodoluminescence (CL). This reflects involvement of different mineralogical, geochemical and geological processes and therefore ion microprobe dating had to be applied. The SHRIMP dating was assisted by CL imaging of the zircon crystals dated. The CL images allowed us, for instance, to distinguish clearly magmatic from metamorphic zircon domains and therefore avoid mixing of ages. Moreover, as is shown below, CL images combined with petrological information led to important conclusions regarding the origin of the zircon domains and the evolutionary history of the rocks.

Overview and geological setting of the H*P*-terrane of the Rhodope zone

The Rhodope zone occupies most of northeastern Greece and southern Bulgaria. It is situated between the Balkan belt to the north and the Dinarides–Hellenides to the south–southwest (Fig. 1). The Balkan belt is a north to northeast vergent thrust belt bounded by the Moesian platform to the north. The Dinarides and Hellenides constitute a predominantly southwest vergent Alpine thrust belt running parallel to the Adriatic coast and the Ionian coast, in a NW–SE direction.

The Rhodope zone is bounded to the west by the Serbomacedonian Massif, a structurally complex domain of predominantly high-grade metamorphic rocks and numerous post-metamorphic granitoids. Radiometric data from the Serbomacedonian Massif (K-Ar and Rb-Sr data on white mica, biotite and hornblende of metamorphic rocks) widely scatter between Hercynian and Alpine ages (Borsi et al. 1965; Harre et al. 1968; Papadopoulos and Kilias 1985). The influence of an Alpine metamorphic event is obvious. The Serbomacedonian Massif is separated from the Rhodope zone by a tectonic contact considered originally as a west-dipping thrust fault of Tertiary age (Kockel and Walther 1965) but reinterpreted recently as a low-angle normal fault formed during middle Miocene to late Pliocene extension (Dinter and Royden 1993). These two geotectonic elements, the Rhodope zone and the Serbomacedonian Massif, lie to the east of the Vardar zone, commonly interpreted as a late Mesozoic to Eocene oceanic suture between Apulia and the southeastern European margin. Burg et al. (1995) suggest that the Serbomacedonian Massif and the Rhodope zone should be considered as a "single major element of the Tethyan orogenic system".

The Rhodope zone consists mainly of rocks of both sedimentary and magmatic origin affected by a high-pressure (eclogite-facies) metamorphism followed by amphibolite-facies and, at least partly, an earlier granulite-facies overprint. Abundant post-metamorphic plutonic and volcanic rocks of Oligocene age crosscut and overly the metamorphic rocks. Distinct tectonic units separated by thrust zones have been recognized in

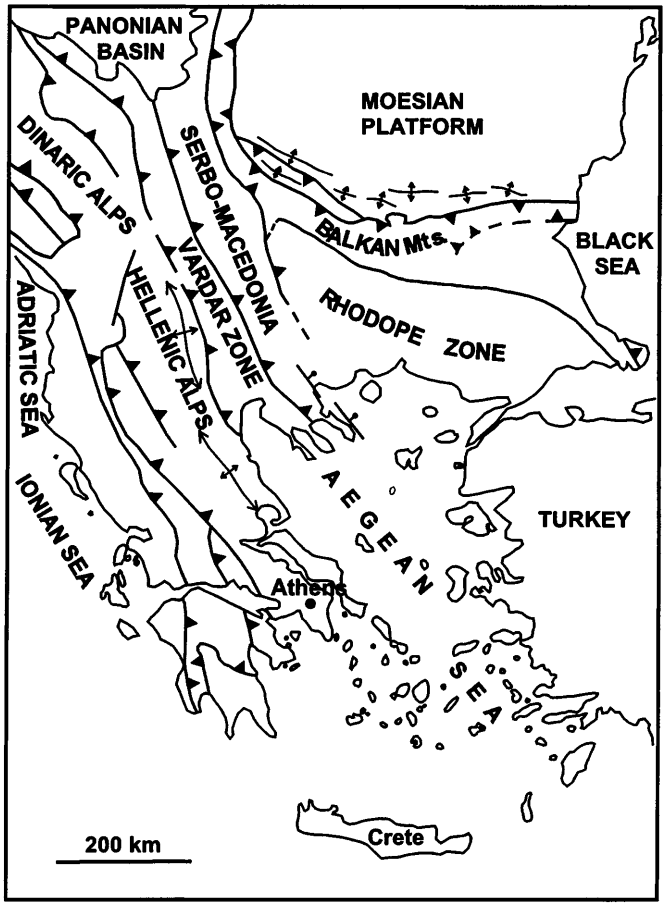

Fig. 1 Sketch map of major tectonic elements in southeastern Europe and northeastern Mediterranean region (from Burchfiel 1980 and Dinter et al. 1995)

the Rhodope: Papanikolaou and Panagopoulos (1981) subdivided the western and central Rhodope zone into an upper unit (Sidironero unit) and a lower unit (Pangaeo unit) separated by an approximately SSE–NNW striking thrust plane. A lower and an upper tectonic unit were recognized also on the basis of abrupt changes of metamorphic grade (referring to the post eclogite-facies overprinting metamorphism), in closely lying rocks (Mposkos 1989). They roughly coincide with the two units suggested by Papanikolaou and Panagopoulos. The lower unit is characterized by metamorphic conditions of upper greenschist to lower amphibolite-facies whereas the upper unit is characterized by medium to upper amphibolite-facies (and, at least partly, granulite-facies). Burg et al. (1996) also recognized an upper and a lower terrane in the Rhodope zone that represent the crystalline footwall and hanging wall of a crustal scale duplex. Several intermediate terranes (thrust units) are stacked between the upper and lower terrane.

In the study area (Fig. 2), which is considered to belong to the upper tectonic unit (in the sense of Mposkos 1989) or to the intermediate terranes (in the sense of Burg et al. 1996), the crystalline basement includes, in order of decreasing abundance, ortho- and paragneisses (migmatized in places), amphibolites (commonly with eclogite relics), marbles, ultramafic and calc-silicate rocks. Metamorphic conditions are $P > 1.9$ GPa, $T > 700$ °C, for the eclogite-facies stage of metamorphism, $T > 800$ °C at $P > 1.5$ GPa for the granulite-facies overprint and $P = 0.8$–1.1 GPa, $T = 580$–690 °C for the amphibolite-facies overprint (Liati and Seidel 1996) (Fig. 9).

Previous geochronological studies on metamorphic rocks of both the Greek and the Bulgarian part of central Rhodope yielded widely scattered and relatively inconclusive data that do, however, indicate an Eocene age for the cooling stages of an Alpine metamorphic event. The K-Ar dating of metamorphic minerals (hornblende, biotite, muscovite) yielded Eocene ages between 36 and 50 Ma, as well as some much older ages, up to 95 Ma, which indicate the presence of excess Ar

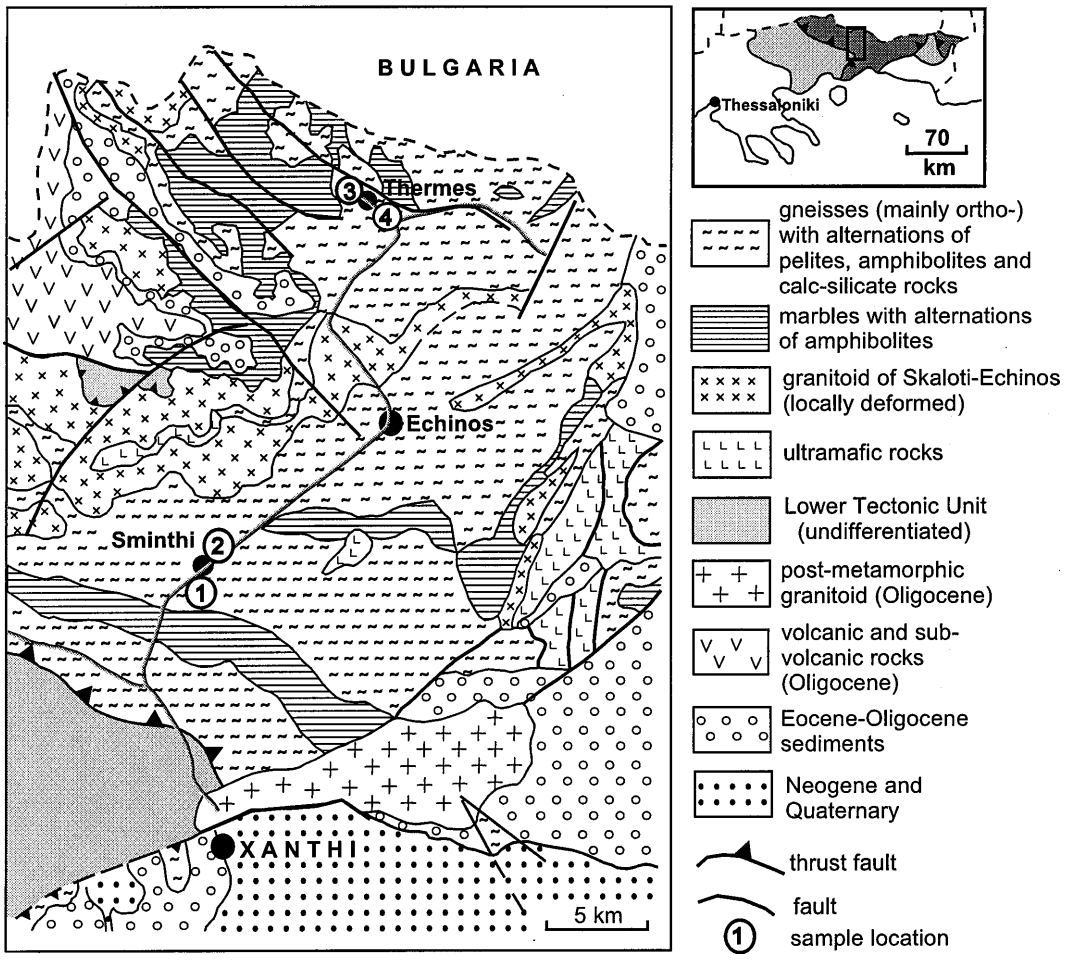

Fig. 2 Generalized geological map of the studied area in central Rhodope, based on a provisional draft by S. Zachos and E. Dimadis (Institute of Geology and Mineral Exploration, Athens). The sample locations for SHRIMP dating are given. In the *inset* map, the *upper* tectonic unit (*light gray*) and *lower* tectonic unit (*dark gray*) in the Greek part of the Rhodope zone are shown. Sample locations: *1* crosscutting pegmatite (RHO12), *2* quartz vein (RHO30), *3* kyanite eclogites (RHO1, RHO3) and orthogneiss (RHO2), *4* leucosome (RHO32)

(Liati 1986; Liati and Kreuzer 1990). The 36–50 Ma ages were interpreted by the above authors to reflect an Eocene amphibolite-facies metamorphic event. The youngest dates in this range of 36–50 Ma should be the closest to a geologically meaningful cooling age, as is usually the case with K-Ar mineral ages in H*P* terranes (e.g., Kelley et al. 1994). A U-Pb monazite age of ca 55 Ma, interpreted as a peak metamorphic age, is reported from a migmatitic gneiss of central Rhodope (Jones et al. 1994). The U-Pb conventional multigrain zircon data ranging from 49 to 58 Ma (outside analytical error limits) are reported from "migmatic pegmatites" of the Bulgarian part of central Rhodope (Arnaudov et al. 1990). Hercynian ages for pre-metamorphic magmatism, are also reported, based on U-Pb conventional zircon dating of an orthogneiss from Thassos island (357 ± 20 Ma; Wawrzenitz 1997), as well as from some metagranitoids (310 ± 5.5 Ma, 319 ± 9 Ma and 305 ± 52 Ma) of the Bulgarian Rhodope zone (Peytcheva and von Quadt 1995).

Field relations and petrography of the dated rocks

Five rock types were chosen for SHRIMP dating of zircon, which were collected in central Rhodope, between Xanthi and Thermes (Fig. 2): (1) an early, deformed quartz vein; (2) kyanite eclogites; (3) leucocratic orthogneiss country rock of the kyanite eclogites; (4) a leucosome from a migmatized orthogneiss; (5) a late, crosscutting pegmatite.

Early, deformed quartz vein

This quartz vein (sample RHO30) is ca 15 cm thick and occurs in paragneisses, in the area of Sminthi (Fig. 2). It lies parallel to the schistosity plane of the paragneisses and is deformed and metamorphosed together with them. Intercalations of calc-silicate rocks occur within the paragneisses.

Under the microscope, quartz grains are elongated and stretched and show sutured boundaries, which indicates intense deformation. Centimeter-thick pockets, found locally in the quartz vein contain the mineral assemblage quartz + clinopyroxene + amphibole + titanite + plagioclase ± calcite. The mineral assemblage of these "pockets" formed during the amphibolite-facies stage of metamorphism. Calcite is secondary and probably formed at even later stages.

Kyanite eclogites

The eclogites studied occur in the area of Thermes (Fig. 2). They form 3–7 m large lenses within the leucocratic orthogneisses. They are overprinted to variable degrees, showing granulite-facies and amphibolite-facies assemblages (Liati and Seidel 1996). Zircons from two eclogite samples (RHO1 and RHO3) from two different lenses were dated.

The eclogites are greenish and commonly contain abundant kyanite and medium- to coarse-grained garnet, up to 2 cm across, typically surrounded by a millimeter-thick black rim of amphibole + plagioclase. The eclogite-facies assemblage is garnet + omphacite + kyanite + zoisite + phengite + rutile ± quartz. Minerals that formed within the granulite-facies are corundum, sapphirine, Fe-Mg-spinel and possibly also högbomite. Various symplectites formed after the granulite-facies overprint in the course of exhumation: (1) clinopyroxene + plagioclase which predominate in the rock matrix, (2) spinel + plagioclase, (3) corundum + plagioclase, (4) biotite + plagioclase, and (5) amphibole + plagioclase (kelyphites). Finally, diablastic amphibole and plagioclase formed within the amphibolite-facies.

Leucocratic orthogneiss country rock of the kyanite eclogites

This rock is medium grained and consists of quartz, plagioclase, K-feldspar and, in lesser proportions, biotite and some green amphibole. No thermobarometric data can be derived from the mineral assemblage of the rock. Critical H*P* minerals have, as yet, not been found. However, the frequent and concordant alternations of all rock types with metabasic rocks containing eclogite relics indicates that the whole sequence has probably undergone the same metamorphic evolution (see also Liati 1986). The leucocratic orthogneiss (sample RHO2) is in direct contact with one of the dated eclogite lenses (sample RHO1).

Leucosome from a migmatized orthogneiss

This folded, ca 7 cm thick leucosome formed within a migmatized orthogneiss in the area of Thermes (sample RHO32). It consists mainly of K-feldspar, plagioclase and quartz with minor biotite. Accessories are orthite and titanite. Embayed to lobate crystal boundaries of quartz, as well as undulatory extinction show that the rock was deformed and incompletely recrystallized.

Late crosscutting pegmatite

This late undeformed pegmatite, which crosscuts the amphibolites, comes from the area south of Sminthi (sample RHO12). It is genetically related to the late stages of metamorphism. It consists of plagioclase, quartz and some K-feldspar, as well as subordinate amphibole, chlorite and titanite. Under the microscope, it shows no signs of deformation.

Analytical procedures

SHRIMP II

Most of the data listed here were obtained on SHRIMP II, at the Australian National University in Canberra. Part of the analyses were carried out on SHRIMP II at the Geological Survey of Canada in Ottawa. Depending on the size of the distinct types of zircon domains, spot sizes between about 8–20 microns were chosen. For data collection, seven scans through the critical mass range were made (Compston et al. 1992).

Cathodoluminescence (CL)

All CL secondary electron (SE) pictures were produced from a split screen on a CamScan CS 4 scanning electron microscope (SEM) at ETH in Zürich operating at 15 kV (Gebauer 1996). The same sample mount was used later for both the CL-SE studies and SHRIMP dating. The SEM is equipped with an ellipsoidal mirror that is located close to the sample within the vacuum chamber and can be adjusted by electro-motors. The sample can thus be located in one focal point while the second focal point lies outside the sample chamber. Here, the CL light enters a highly sensitive photo multiplier through a quartz glass – vacuum window and a light channel. The signal of the photo multiplier is then used to produce the CL picture via a video-amplifier. The SE pictures were produced simultaneously together with the CL pictures using a different detector. In general, strong CL means high amounts of minor and trace elements, weak CL means low amounts of minor and trace elements, including U. Thus, the relative U contents can qualitatively be predicted via CL.

Data evaluation

For the calculation of the Pb/U ratios, the data were corrected for common Pb using the ^{207}Pb correction method. Since this correction is based on the assumption of concordance, the data are graphically presented not on a Concordia but on a Tera-Wasserburg (TW) diagram.

The amount of common Pb was calculated using the isotope composition of common Pb obtained from both the model of Cumming and Richards (1975) and using the Broken Hill common Pb composition. With the exception of samples with very low $^{206}Pb/^{204}Pb$ ratios, the resulting ages were analytically indistinguishable. However, the Cumming and Richards model was chosen here, since most analyzed spots plot in the TW diagram along a mixing line closer to this isotopic composition ($^{207}Pb/^{206}Pb$ = 0.835, for Alpine ages). The individual data points are plotted with 2σ errors.

The mean ages were calculated both as normal mean and weighted mean. Although in both cases the resulting ages are almost identical, the weighted mean is preferred here because it is more representative of the analytically best measurements. Mean ages are given at the 95% confidence level. For single analyses (Table 1), the 1σ error is given.

CL patterns and morphology of zircons

The *early deformed quartz vein* within the paragneisses contains hydrothermally formed zircons, as well as detrital zircons derived from the country rock. The hydrothermal zircons were chosen for dating. They are generally elongated (length/width: 5:1) and show oscillatory euhedral growth zoning (Fig. 3). In some cases, narrow CL-bright rims are observed around the oscillatory hydrothermal domains (Fig. 3C, D). As discussed below, this reflects resetting of the U-Pb zircon system at the *T*-peak.

In the *kyanite eclogites*, the zircons are generally prismatic and euhedral, as typically observed for crystals precipitated from a melt (Fig. 4). Their relatively large size indicates that the protolith of the eclogites is very probably of gabbroic origin, since such co-magmatic zircons cannot grow from the rapidly cooling basaltic melts. Atypical for eclogite zircons derived from intrusive protoliths are their CL characteristics. The oscillatory, euhedral growth zoning usually observed in zircons of gabbroic rocks can only rarely and then only very faintly be observed. Instead, there are relatively large areas with homogeneous CL intensities and some faded fir tree and sector zoning patterns. The U contents and especially Th contents are generally very low resulting in very low Th/U ratios (0.006–0.029; Table 1).

Interaction of fluids with the recrystallizing zircons in the course of metamorphism may best explain these unusual observations, that is fading and disappearance of oscillatory zoning, very low U contents and Th/U ratios, as well as predominantly completely reset ages (see below, section 7.2). Fluids were present in these rocks during both prograde metamorphism close to the *P*-peak (eclogite-facies), as well as during decompression related metamorphic overprinting.

In the *orthogneiss* country rock of the kyanite eclogites, prismatic, euhedral zircon grains are observed. In their central parts they exhibit oscillatory zoning, typical for zircons precipitated from a granitic melt (Fig. 5). As usually observed for gneisses that exceed amphibolite-facies metamorphic conditions, the magmatic zircons started to recrystallize at their rims. As a result, oscillatory zoning fades progressively until, in CL, an almost homogeneous looking, bright rim is observed around the magmatic core. The outer limits of these metamorphic zircon domains are identical to those of the previous fully magmatic, euhedral zircons. The inner boundary to the oscillatory, magmatic zircon cores is irregular. Commonly, intermediate stages with ghost zoning are preserved. Identical outer limits of the zircon rims to those of the magmatic domain, as well as progressive fading of oscillatory zoning argues against new growth of zircon during metamorphism. The formation of zircon 5B shows some peculiarities discussed below, in combination with the SHRIMP results.

The leucosome of a migmatized orthogneiss contains zircons identical to those of the enclosing orthogneiss described above, but also contains euhedral fully oscillatory zoned zircons without CL-bright rims (compare Figs. 5 and 6). The latter obviously crystallized from the partial melt that formed by decompressional melting of the orthogneiss and gave rise to the leucosome.

The zircons of the *crosscutting pegmatite* have shape and CL characteristics similar to those commonly observed in such rocks. The originally euhedral crystals are externally corroded and internally altered (Fig. 7). The domains of the zircon crystals analyzed contain between ca 2000 and 7000 ppm U (see below).

Results of SHRIMP dating and interpretation

The ion microprobe data for the analyzed zircons are given in Table 1 and plotted on Tera-Wasserburg diagrams for each rock type (Fig. 8). The weighted mean ages and the errors (given at the 95% confidence level) are summarized in Table 2.

Early deformed quartz vein

Eight data points were obtained from the hydrothermally formed, oscillatory domains of the zircon crystals. On a TW diagram they plot on a mixing line with common Pb and radiogenic $^{238}U/^{206}Pb$ as end members (Fig. 8A) and yield a weighted mean age of 45.3 ± 0.9 Ma. Based on their form and CL characteristics (see above), the zircon crystals must have precipitated from a fluid, in this case an early hydrothermal fluid. This hydrothermal fluid is responsible for the formation of the quartz vein, at low or very low grade conditions. The age of 45.3 ± 0.9 Ma is interpreted to reflect the time of formation of the quartz vein. As discussed below, these veins have indeed formed signifi-

Table 1 U, Th, Pb SHRIMP data for zircons from metamorphic rocks of central Rhodope (for samples in *italics* see text)

Sample	U (ppm)	Th (ppm)	Th/U	Radiogenic Pb (ppm)	f^{206}Pb (%)	^{207}Pb/^{206}Pb (1σ) (uncorrected)	^{238}U/^{206}Pb (1σ) (uncorrected)	^{206}Pb/^{238}U (1σ)	Age (Ma) ^{206}Pb/^{238}U (1σ)
Prograde quartz vein									
RHO30-2.1	647	2.69	0.004	3	14.7	0.1626 ± 0.0064	127.9 ± 2.7	0.0067 ± 0.0002	42.9 ± 1.0
RHO30-3.2	548	3.01	0.005	4	4.4	0.0884 ± 0.0056	126.0 ± 6.5	0.0076 ± 0.0002	48.3 ± 1.2
RHO30-3.3	465	2.12	0.005	3	10.5	0.1456 ± 0.0113	123.3 ± 5.8	0.0073 ± 0.0002	45.6 ± 1.1
RHO30-4.1	188	1.27	0.007	1	6.0	0.1029 ± 0.0112	128.9 ± 8.5	0.0073 ± 0.0002	46.3 ± 1.5
RHO30-6.1	612	4.02	0.007	4	2.7	0.0685 ± 0.0055	135.8 ± 6.2	0.0072 ± 0.0002	46.0 ± 1.1
RHO30-6.2	781	5.09	0.007	5	3.5	0.0749 ± 0.0034	137.2 ± 6.3	0.0070 ± 0.0002	45.2 ± 1.1
RHO30-6.3	772	5.57	0.007	6	5.6	0.0910 ± 0.0049	136.8 ± 5.9	0.0069 ± 0.0002	44.4 ± 1.0
RHO30-7.1	402	1.90	0.005	3	6.7	0.0998 ± 0.0070	132.6 ± 6.2	0.0058 ± 0.0005	45.2 ± 1.1
RHO30-3.1	*327*	*0.95*	*0.003*	*13*	*62.1*	*0.5367 ± 0.0266*	*62.2 ± 2.1*	*0.0077 ± 0.0005*	*39.2 ± 3.7*
RHO30-2.2	*310*	*0.53*	*0.002*	*2*	*8.3*	*0.1249 ± 0.0188*	*156.5 ± 14.2*	*0.0059 ± 0.0003*	*37.0 ± 1.7*
RHO30-2.3	*334*	*0.48*	*0.001*	*2*	*22.2*	*0.2556 ± 0.0287*	*131.0 ± 11.5*	*0.0059 ± 0.0003*	*36.1 ± 1.7*
Eclogites									
RHO1-6.1	59	1.72	0.029	< 1	10.6	0.1416 ± 0.0122	131.9 ± 7.1	0.0068 ± 0.0004	43.5 ± 2.5
RHO1-6.2	64	1.56	0.024	< 1	4.9	0.0971 ± 0.0050	149.8 ± 3.4	0.0064 ± 0.0002	40.8 ± 1.0
RHO1-9.1	65	1.10	0.017	< 1	22.1	0.2310 ± 0.0109	119.4 ± 4.9	0.0065 ± 0.0003	41.9 ± 1.9
RHO1-9.2	56	0.42	0.007	< 1	< 1	0.0579 ± 0.0046	158.3 ± 4.6	0.0063 ± 0.0002	40.7 ± 1.2
RHO1-9.3	66	0.38	0.006	< 1	< 1	0.0636 ± 0.0056	151.6 ± 4.0	0.0066 ± 0.0002	42.2 ± 1.1
RHO1-9.4	72	0.58	0.008	< 1	1.2	0.0687 ± 0.0046	149.7 ± 3.9	0.0066 ± 0.0002	42.4 ± 1.1
RHO1-7.1	57	0.52	0.009	1	43.9	0.3998 ± 0.0168	80.56 ± 2.3	0.0070 ± 0.0003	44.8 ± 2.1
RHO1-7.2	59	1.35	0.023	< 1	1.16	0.0681 ± 0.0043	150.5 ± 5.2	0.0066 ± 0.0002	42.2 ± 1.5
RHO1-4.1	52	0.48	0.009	< 1	< 1	0.0545 ± 0.0048	146.9 ± 3.7	0.0069 ± 0.0002	44.0 ± 1.2
RHO1-10.1	*25*	*9.48*	*0.386*	*1*	*< 1*	*0.4585 ± 0.0307*	*63.0 ± 3.3*	*0.0077 ± 0.0008*	*49.5 ± 4.8*
RHO1-10.2	*237*	*136*	*0.574*	*4*	*< 1*	*0.0748 ± 0.0030*	*81.2 ± 1.6*	*0.0121 ± 0.0003*	*77.4 ± 4.8*
RHO3-5.1	33	0.80	0.024	< 1	< 1	0.0524 ± 0.0059	152.1 ± 4.6	0.0066 ± 0.0002	42.6 ± 1.3
Orthogneiss (*Alpine zircon domains*)									
RHO2-1.2	530	3.24	0.006	3	2.3	0.0769 ± 0.0043	147.3 ± 7.6	0.0066 ± 0.0002	42.6 ± 1.1
RHO2-2.1	413	1.48	0.004	2	4.3	0.0926 ± 0.0064	146.4 ± 7.9	0.0065 ± 0.0002	42.0 ± 1.2
RHO2-5.1	39	0.01	0.002	< 1	17.1	0.1917 ± 0.0258	134.0 ± 17.8	0.0062 ± 0.0004	39.8 ± 2.8
RHO2-6.1	1409	8.75	0.006	9	< 1	0.0608 ± 0.0028	151.9 ± 6.8	0.0066 ± 0.0002	42.2 ± 0.9
RHO2-6.2	2402	12.45	0.005	15	< 1	0.0549 ± 0.0015	152.0 ± 6.8	0.0066 ± 0.0002	42.5 ± 1.0
RHO2-6.3	411	2.17	0.005	2	5.7	0.1030 ± 0.0109	148.1 ± 9.9	0.0064 ± 0.0002	40.9 ± 1.4
RHO2-8.1	37	0.24	0.007	< 1	37.0	0.3463 ± 0.0342	100.7 ± 9.4	0.0063 ± 0.0004	40.2 ± 2.3
RHO2-13.1	35	0.23	0.007	< 1	38.1	0.3552 ± 0.0337	101.2 ± 9.0	0.0061 ± 0.0004	39.3 ± 2.2
(*Hercynian zircon domains*)									
RHO2-5.2	294	100	0.341	14	< 1	0.0633 ± 0.0024	22.3 ± 1.1	0.0446 ± 0.0011	281 ± 7
RHO2-5.3	626	168	0.269	30	< 1	0.0561 ± 0.0011	21.0 ± 0.9	0.0478 ± 0.0011	301 ± 7
RHO2-13.3	2534	618	0.244	115	< 1	0.0543 ± 0.0006	22.1 ± 1.0	0.0456 ± 0.0011	288 ± 7
RHO2-10.1	1030	651	0.631	53	< 1	0.0560 ± 0.0010	21.2 ± 0.9	0.0474 ± 0.0010	298 ± 6
RHO2-10.2	475	77	0.162	22	< 1	0.0585 ± 0.0020	20.8 ± 1.0	0.0482 ± 0.0011	303 ± 7
Leucosome in migmatized orthogneiss									
RHO32-2.1	1551	6.9	0.004	9	2.4	0.0661 ± 0.0029	158.4 ± 6.0	0.0062 ± 0.0001	39.6 ± 0.8
RHO32-3.1	1987	5.9	0.003	11	1.5	0.0590 ± 0.0024	159.2 ± 5.7	0.0062 ± 0.0001	39.7 ± 0.7
RHO32-5.1	1447	6.9	0.005	8	2.1	0.0635 ± 0.0039	155.6 ± 5.4	0.0063 ± 0.0001	40.4 ± 0.7
RHO32-10.1	2031	6.9	0.0034	11	1.6	0.0595 ± 0.0030	157.4 ± 5.6	0.0062 ± 0.0001	40.2 ± 0.7
Crosscutting pegmatite									
RHO12-1.1	163	21	0.127	1	8.6	0.1150 ± 0.0171	168.8 ± 11.5	0.0054 ± 0.0002	34.8 ± 1.3
RHO12-3.1	504	14	0.028	3	2.6	0.0675 ± 0.0104	169.7 ± 9.6	0.0057 ± 0.0002	36.9 ± 1.1
RHO12-3.2	744	17	0.023	4	20.5	0.2087 ± 0.0138	142.9 ± 8.4	0.0056 ± 0.0002	35.8 ± 1.1
RHO12-6.1	1862	138	0.074	10	1.2	0.0561 ± 0.0030	172.3 ± 6.9	0.0057 ± 0.0001	36.9 ± 0.7
RHO12-7.1	1460	51	0.035	7	7.1	0.1025 ± 0.0109	170.8 ± 11.2	0.0054 ± 0.0002	35.0 ± 1.1
RHO12-4.1	2066	63	0.030	14	< 1	0.0501 ± 0.0008	139.2 ± 2.3	0.0073 ± 0.0001	46.0 ± 0.8
RHO12-6.2	2763	188	0.068	16	< 1	0.0519 ± 0.0012	158.6 ± 1.8	0.0063 ± 0.0001	40.3 ± 0.5
RHO12-6.3	2347	119	0.051	14	< 1	0.0486 ± 0.0011	157.1 ± 2.0	0.0063 ± 0.0001	40.8 ± 0.5
RHO12-7.2	7081	335	0.047	42	1.7	0.0605 ± 0.0011	150.3 ± 7.1	0.0065 ± 0.0003	42.0 ± 2.0

cantly earlier than both the *P*- and *T*-peak of metamorphism (see Fig. 9, *P-T-t* path). The *PT* conditions of formation of this early deformed quartz vein are uncertain. However, ca 250–300 °C, 0.3 GPa can be considered as the most likely conditions, as most quartz veins form during prograde metamorphism at this range of *PT* (e.g., McNamara 1965), as a consequence of dehydration reactions in siliceous metasediments and dissolution of quartz in the aqueous fluid (e.g., Manning 1996). In any case, as is discussed below (section 9) even if the quartz vein formed at higher *PT*, this has a negligible effect on calculated burial and heating rates.

Three spots on the bright narrow rims around the oscillatory domain of two zircon crystals from this

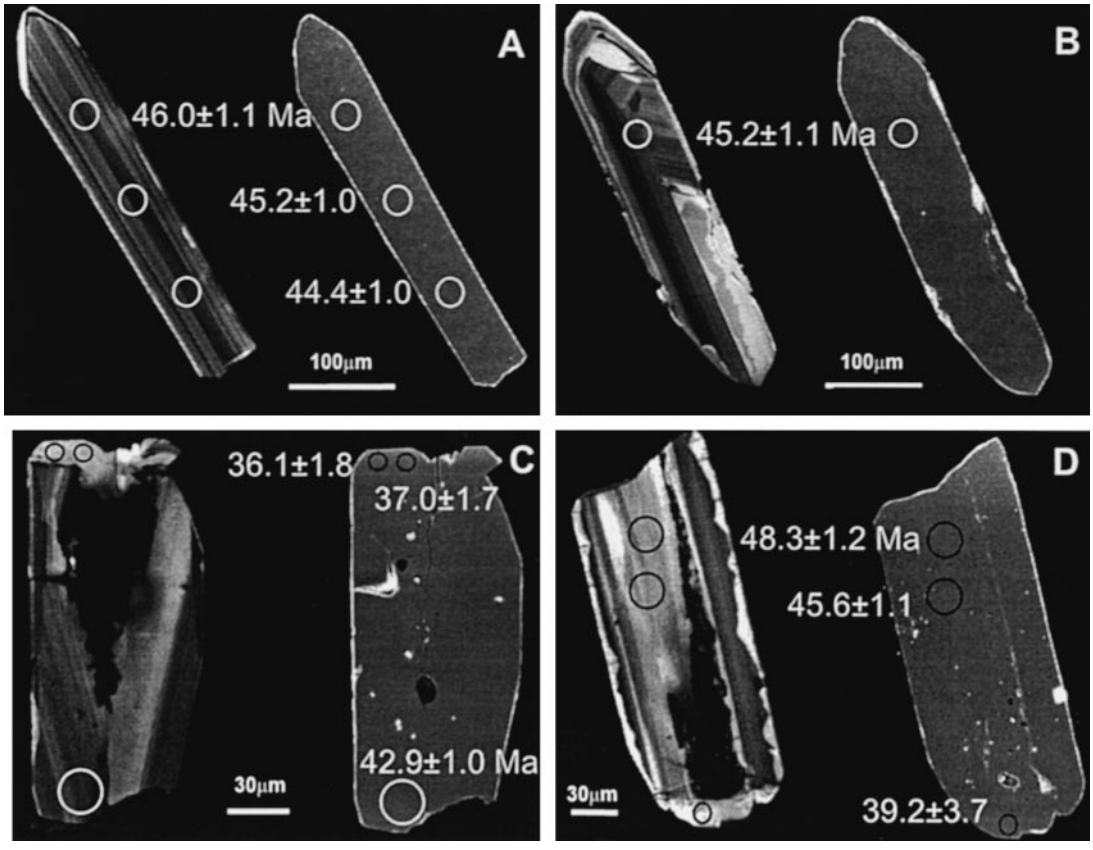

Fig. 3A–D Cathodoluminescence (CL) pictures (on the *left*) and secondary electron (SE) pictures (on the *right*) of zircon crystals from the early deformed quartz vein: **A** zircon RHO30-6; **B** zircon RHO30-7; **C** zircon RHO30-2; **D** zircon RHO30-3. Note oscillatory, euhedral growth zoning, typical for crystals precipitated from a melt or a fluid (here hydrothermal fluid). Note also *narrow bright rims* in **C** and **D**

quartz vein (Fig. 3C, D; samples in italics of Table 1) lie on a mixing line (Fig. 8A) with a lower intercept age of 36.8 ± 5.0 Ma. The large error of 5 Ma is mainly due to the small number of analyses (three). This young age obviously reflects resetting of the U-Pb zircon system during a subsequent stage of metamorphism of the quartz vein at peak temperature conditions (see below).

Kyanite eclogites

Ten data points were obtained from the eclogite zircons and yielded a weighted mean age of 42.2 ± 0.9 Ma. On a TW diagram, they all plot on a mixing line (Fig. 8B). No protolith age could be identified since almost no original magmatic domains are preserved. However, some domains were found that exhibit higher U contents

Fig. 4A, B CL pictures (on the *left*) and SE pictures (on the *right*) of zircon crystals from the kyanite eclogites: **A** zircon RHO1-9; **B** zircon RHO1-10. Oscillatory and euhedral growth zoning can faintly be observed. Note that the analyzed points in **B** lie partly within an older core (*darker*)

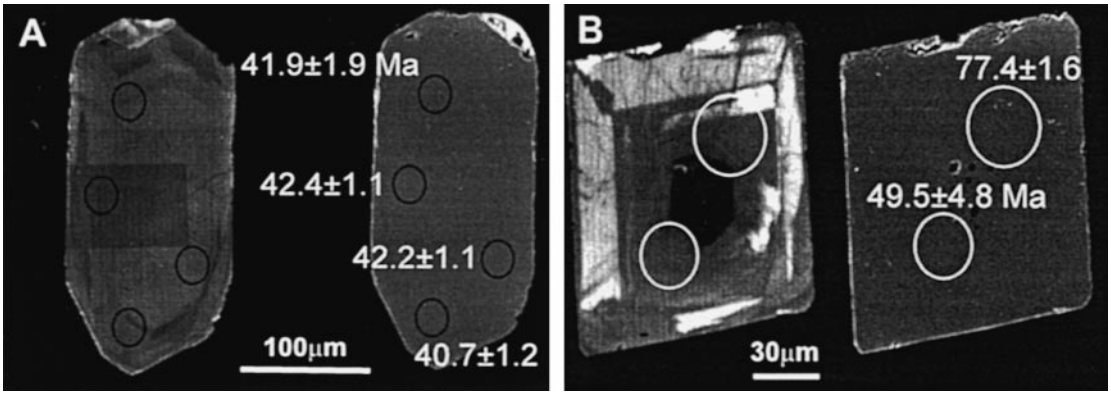

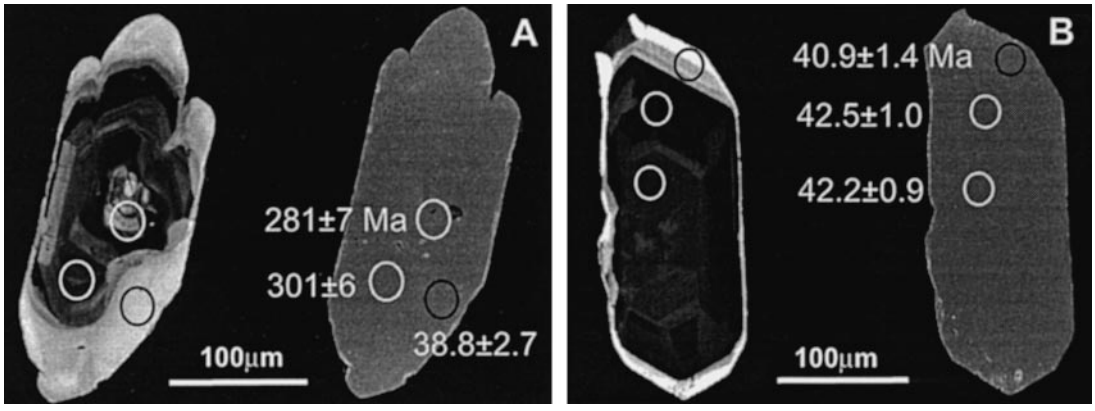

Fig. 5A, B CL pictures (on the *left*) and SE pictures (on the *right*) of zircon crystals from the orthogneisses containing eclogite boudins: **A** zircon RHO2-5; **B** zircon RHO2-6. In **A** zircon shows a Hercynian oscillatory zoned magmatic core and an Eocene, homogeneous looking, *bright*, metamorphic *rim*. In **B** Eocene ages from all over the crystal indicate that the whole zircon grain formed intergranularly during incipient partial melting or complete Pb loss from the Hercynian zircon during metamorphism

up to 237 ppm, higher Th/U ratios up to 0.57, as well as pre-metamorphic Pb components resulting in apparent $^{206}Pb/^{238}U$ ages of 49.5 Ma and 77.4 Ma (e.g., Fig. 4B; samples in italics of Table 1, not included in the age calculation). The highest age (77.4 Ma) must therefore be considered as the minimum age of the gabbroic protolith of the eclogites near Thermes.

As mentioned above, the shape of the zircons and their rather homogeneous CL patterns indicates that metamorphic fluids, liberated close to the *P*-peak (see below) interacted with the crystal lattice of the recrystallizing zircon. For the majority of the analyzed spots radiogenic Pb was leached, thus resetting the primary magmatic zircon ages. Besides radiogenic Pb, Th and U were also partly removed from these zircons. This impoverishment of the zircon in mainly Th, but also U and probably other trace elements, is reflected in its CL characteristics (fading of oscillatory zoning and a nearly homogeneous appearance). Leaching of Pb, Th and sometimes also U in a fluid rich environment with (or even without) fading of oscillatory zoning has been reported before (e.g., Vavra et al. 1996; Gebauer 1996; Gebauer et al. 1997). This is a different process compared to the one that operates in the early deformed quartz vein, where fluids were also involved, but at much lower temperatures. In the case of the quartz vein, completely new zircon crystals first precipitate from a hydrothermal fluid and, as is usually the case with zircon crystals precipitated from a melt or aqueous fluid, exhibit oscillatory zoning.

The 42.2 ± 0.9 Ma age should therefore date the time of the metamorphic reaction(s) that led to fluid generation, interaction with existing magmatic zircon and complete resetting of primary (protolith) ages. Two possibilities are envisaged in this respect: (1) The reacting fluids are related to the H_2O-producing reactions during advanced stages of prograde metamorphism. Such reactions, which definitely occurred in the eclogites, are the breakdown reaction of zoisite (zoisite = grossular + kyanite + quartz + H_2O) and the breakdown reaction of paragonite (paragonite = jadeite + kyanite + H_2O). The latter is the last prograde H_2O-liberating reaction and took place at

Fig. 6A, B CL pictures (on the *left*) and SE pictures (on the *right*) of zircon crystals from the leucosome of a migmatized orthogneiss: **A** zircon RHO32-2; **B** zircon RHO32-3. Note oscillatory zoning and planar crystal faces, features typical for zircons precipitated from melt or a fluid (here partial melt). Note also the absence of *bright rims* (compare with orthogneiss zircons of Fig. 5)

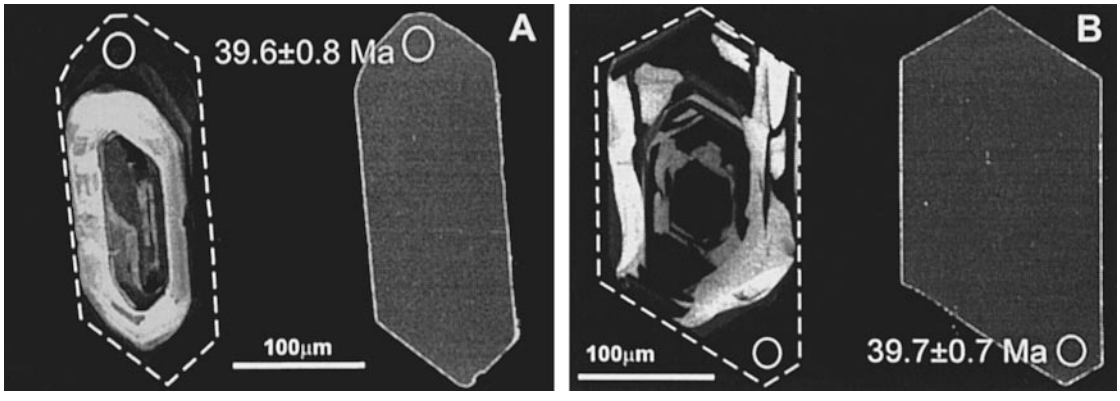

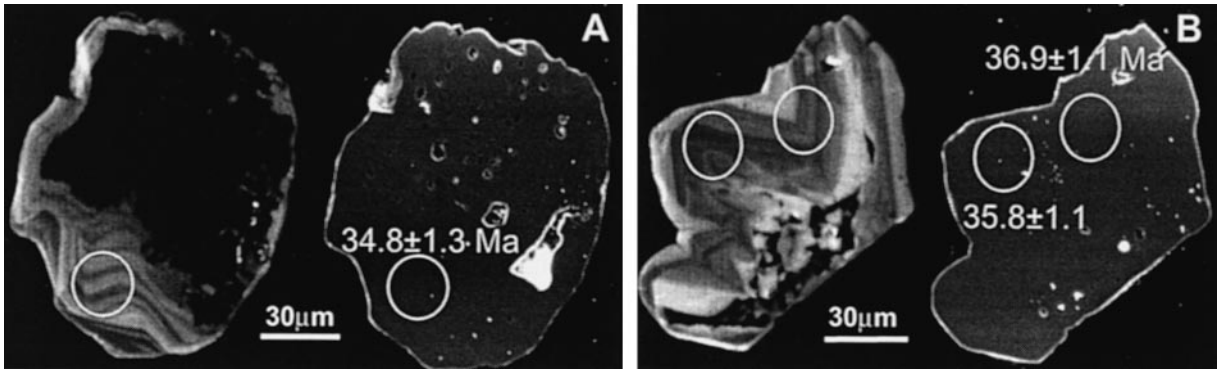

Fig. 7A, B CL pictures (on the *left*) and SE pictures (on the *right*) of zircon crystals from the crosscutting pegmatite: **A** zircon RHO12-1; **B** zircon RHO12-3. Note external corrosion and internal alteration, CL characteristics typically observed in zircons of such rocks

minimum *PT* conditions of 1.9 GPa, 700 °C (Liati and Seidel 1996). These are probably close to the peak conditions of the eclogite-facies metamorphism. The zircon ages would then reflect a prograde stage of metamorphism which would closely approximate the time of peak pressures. (2) The reacting fluids are related to H_2O-liberating reactions related to the decompression stage, during the granulite-facies metamorphic overprint, close to the *T*-peak (e.g., breakdown of phengite: phengite + garnet = biotite + plagioclase + H_2O; see also Heinrich 1982). In this case, the 42.2 ± 0.9 Ma age would reflect the initiation of hydration of the eclogites during decompression. As discussed below, in view of the age results obtained from the leucosome and the orthogneisses, the first case is favored.

Orthogneiss country rock of the kyanite eclogites

Five out of seven analyses on oscillatory zoned cores (primary magmatic domains) of zircons from this orthogneiss plot on a mixing line that intersects the concordia at 294 ± 8 Ma (Fig. 8C). The protolith of this rock was therefore a Hercynian granite. Two spot analyses plot off the mixing line, namely one on the right side (indicating Pb loss) and one of the left side (indicating an older Pb component). The latter is explained by the fact that the analyzed spot lies partly on an older core recognised in CL.

The Hercynian magmatic zircon crystals have partly recrystallized and lost all their radiogenic Pb during Alpine metamorphism, as indicated by the presence of rims bright in CL around the oscillatory zoned magmatic domains and the crystal form characteristics. No new growth took place (see section 6). Eight spot analyses were obtained from these completely reset metamorphic domains. In a TW diagram (Fig. 8D) they lie on a mixing line that intersects the concordia at 42.0 ± 1.1 Ma. This age compares well with that obtained from the eclogite zircons. It is therefore evident that the geochronological data support the view that the orthogneisses have been metamorphosed "in situ" with the enclosing eclogites and contradict the assumption of later tectonic emplacement of the eclogites. One of the zircon crystals analyzed (Fig. 5B) yielded only Alpine ages at both the innermost oscillatory domains, dark in CL, and the bright rims. One possible interpretation is that the whole zircon grain formed intergranularly during incipient partial melting (compare with leucosome zircons and see also section 8, below). Alternatively, complete lead loss from the Hercynian zircon may have occurred during metamorphism.

Leucosome in a migmatized orthogneiss

Four spots were analyzed on the oscillatory zoned zircons which obviously crystallized from the partial melt during migmatization. On a TW diagram (Fig. 8E) they all plot on a mixing line and yield a weighted mean age of 40.0 ± 1.0 Ma. This age reflects the time of zircon crystallization from the partial melt. This can further be interpreted as the time that the rocks experienced the highest temperatures ($T > 800$ °C, $P > 1.5$ GPa). However, if we take into consideration the favoring role of fluids, derived by dehydration reactions, in partial melting processes, the leucosome formation may be related not only to high prevailing temperatures but also to the presence of fluids triggering melting. Therefore, the 40 ± 1.0 Ma age most probably represents the time of the temperature peak and melt generation (migmatization).

A comparison with the age obtained from the eclogite zircons (42.2 ± 0.9 Ma) shows that the leucosome formed 2.2 ± 1.9 Ma later. The 1.9 Ma error is the maximum error obtained if we assume the rather unlikely case that the extreme age values apply simultaneously for the eclogites and the leucosome. Thus, if we take the extreme error margins for the ages obtained for the eclogite and the leucosome, the maximum and minimum age difference becomes 4.1 Ma and 0.3 Ma, respectively. Thus, there is no overlapping of these two ages at the 95% confidence level. Moreover, the weighted mean error of 1.0 Ma for the leucosome is relatively large and possibly not representative, due to the few – but analytically very consistent – data spots. If

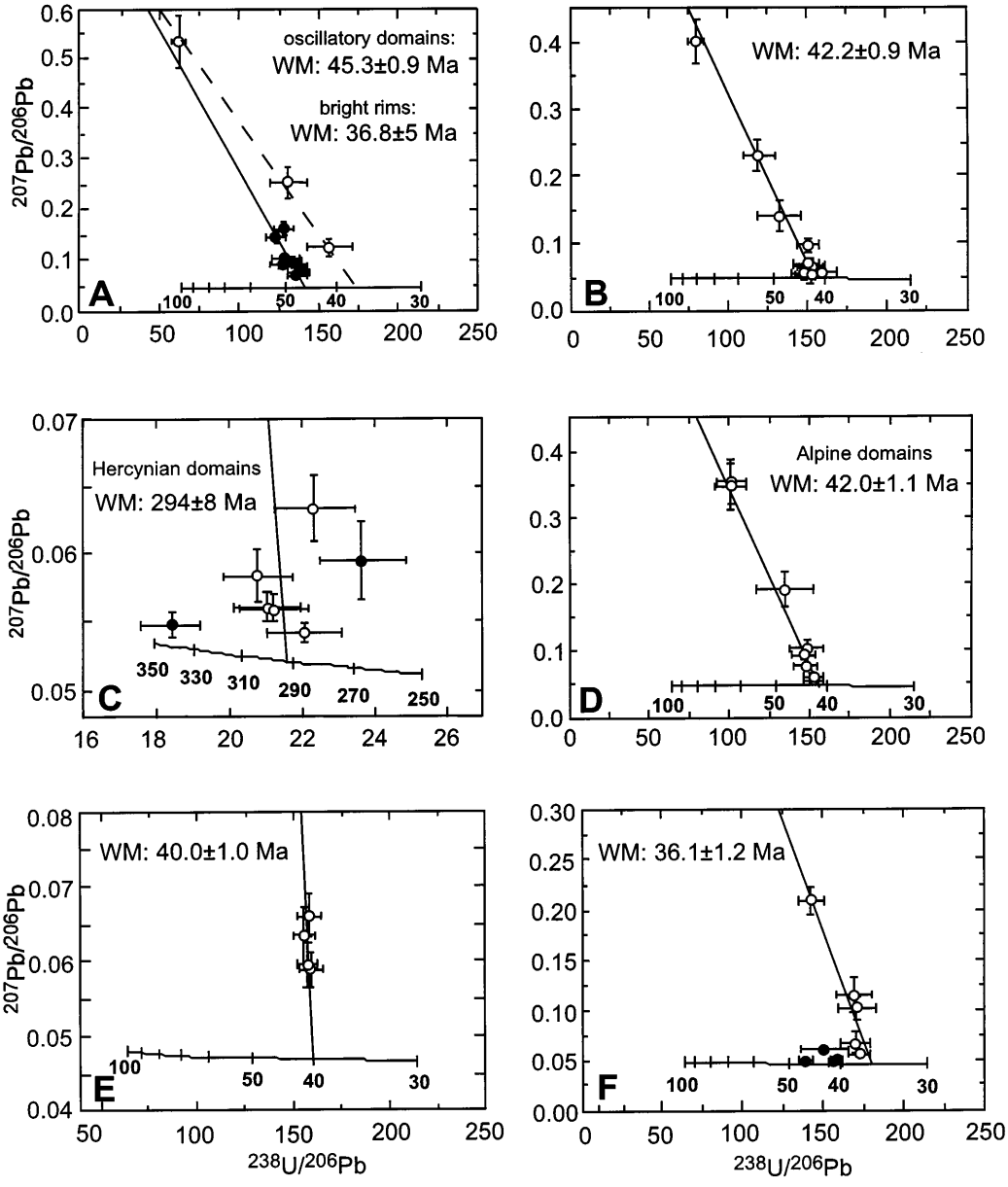

Fig. 8A–F Tera-Wasserburg (TW) diagrams with data obtained on zircons from: **A** the early deformed quartz vein; (*filled circles* data from the hydrothermal, oscillatory domains of the zircon crystals, *open circles* data from the narrow, bright metamorphic rims of the zircons); **B** the eclogites; **C** and **D** the orthogneisses: In **C** *filled circles* on the *left* and *right* side of the mixing line correspond to analyzed points with an older Pb component and Pb loss, respectively. **E** the leucosome and **F** the crosscutting pegmatite; *filled circles* that plot *off* the mixing line correspond to analyzed spots with U contents higher than 2000 ppm (samples in italics of Table 1). The analyzed points plot along a mixing line with common Pb (composition according to the model of Cumming and Richards) and radiogenic $^{238}U/^{206}Pb$ as end members. (*WM* weighted mean). Error *bars* are 2σ errors

we consider the normal mean values and errors of the leucosome (40.0 ± 0.6 Ma) and the eclogite zircons (42.5 ± 0.9 Ma), the maximum age difference becomes 2.5 Ma with a maximum error of 1.5 Ma, which increases the minimum age difference from 0.3 Ma to 1.0 Ma. In any case, the 42.2 Ma and the 40.0 Ma ages must be considered as two statistically distinct ages related to separate stages of the metamorphic evolution.

Crosscutting pegmatite

Five spot data obtained from zircons of the crosscutting pegmatite plot on a mixing line in the TW diagram of Fig. 8F. They yield a weighted mean age of 36.1 ± 1.2 Ma which is interpreted to reflect the intrusion of this rock into the upper crust, with ambient temperatures of ca 300 °C, at a depth of ca 10 km. This is supported by a biotite K/Ar cooling age of 35.8 ± 0.3 Ma reported for a migmatite of the same area (Liati 1986; Liati and Kreuzer 1990).

Another four spots analyzed from the pegmatite zircons showed very high U contents, up to 7000 ppm (Table 1, samples in italics). They yielded inconsistently

Table 2 Mean SHRIMP ages (Ma) of zircon domains from the dated rocks of central Rhodope (*c.l.* confidence level)

Sample	Weighted mean ±error (95% c.l.)	CL-type of zircon domain
Early qz-vein (RHO30) (8 spots)	45.3 ± 0.9	Oscillatory zoning
Early qz-vein (RHO30) (3 spots)	36.8 ± 5.0	Narrow bright rim
Eclogite (RHO1, RHO3) (10 spots)	42.2 ± 0.9	Faded oscillatory zoning
Orthogneiss (RHO2) (5 spots)	294 ± 8	Oscillatory zoning
Orthogneiss (RHO2) (8 spots)	42.0 ± 1.1	Bright rim
Leucosome (RHO32) (4 spots)	40.0 ± 1.0	Oscillatory zoning
Pegmatite (RHO12) (5 spots)	36.1 ± 1.2	Oscillatory zoning

higher ages which plot off the mixing line in the TW diagram (Fig. 8F) and were neglected in the age calculation. It is a common case in SHRIMP data that analyses with U contents higher than ca 2000 ppm may be erroneous and should not be considered in the age calculation (see also Mc Laren et al. 1994; Williams et al. 1996).

P-T-t path and correlation with the SHRIMP results

The ages obtained from SHRIMP analyses of different zircon domains from the dated rocks of central Rhodope allow to infer four distinct stages within an Alpine metamorphic cycle: at 45.3 ± 0.9 Ma, at 42.2 ± 0.9 Ma,

Fig. 9 *P-T-*$t_{(absolute)}$ path for the rocks of the upper tectonic unit of central Rhodope (based on the *P-T-*$t_{(relative)}$ path from Liati and Seidel 1996). Fields (*1*) and (*2*) represent the range of *P-T* conditions using the garnet-hornblende geothermometer of Graham and Powell (1984) and the garnet-amphibole-plagioclase-quartz geobarometer of Kohn and Spear (1989) (only for field 2); (*3*) represents the minimum *PT* conditions for the peak eclogite-facies stage; (*4*) represents *PT* of the overprinting granulite-facies stage inferred by the presence of sapphirine and of albite$_{50-67}$ + corundum forming as reaction products of jadeite$_{50}$ + kyanite; field (*5*) represents the range of *PT* conditions of the amphibolite-facies stage using the garnet-hornblende geothermometer and the garnet-amphibole-plagioclase-quartz geobarometer, as above. The shape of the *PT* trajectory between the minimum peak *PT* conditions during prograde metamorphism (field 3) and the estimated post-pressure peak exhumation conditions (field 4) is uncertain, due to lack of petrological data and is drawn *dashed*. The biotite age of 35.8 Ma is from a migmatite in the area of Echinos (Liati 1986; Liati and Kreuzer 1990)

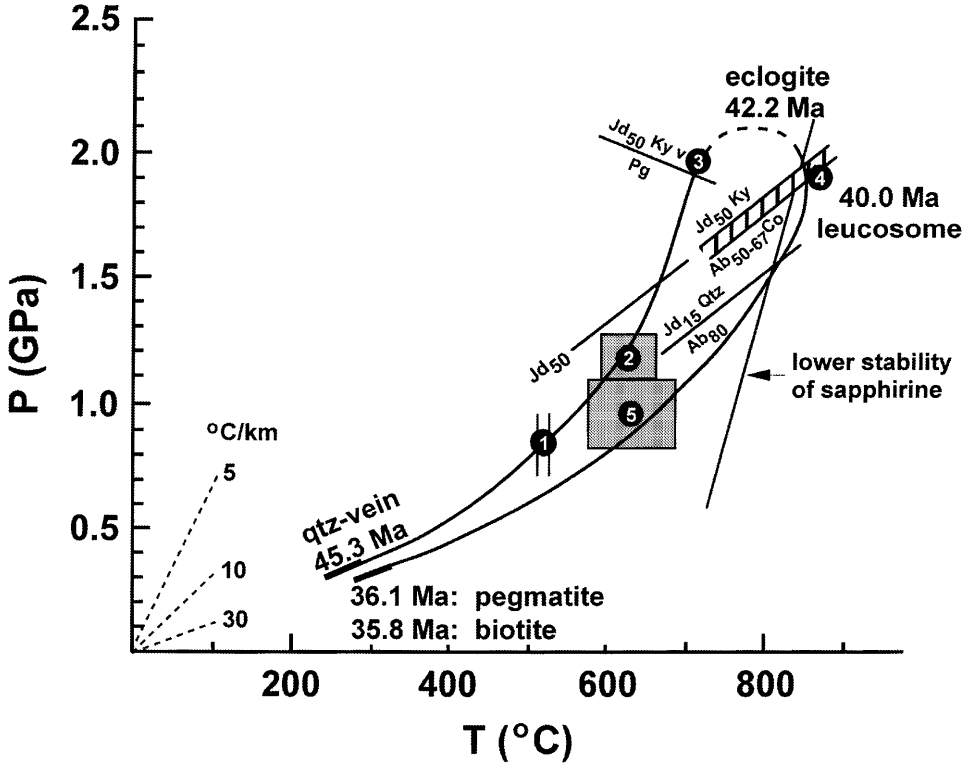

at 40.0 ± 1.0 Ma and at 36.1 ± 1.2 Ma. The 45.3 ± 0.9 Ma and the 36.1 ± 1.2 Ma ages are clearly connected with the early stages of subduction (prograde metamorphism) and final stages of exhumation (retrograde metamorphism), respectively. Thus, the whole metamorphic cycle between the early and late stages (above ca 300 °C, 0.3 GPa) lasted 9.2 ± 2.1 Ma. The 2.1 Ma error is the maximum error obtained if we assume the rather unlikely case that the extreme age values apply simultaneously for the early quartz vein and the pegmatite.

The 40.0 ± 1.0 Ma age corresponds to the time that the rocks experienced the highest temperatures. At this time partial melting and leucosome formation occurred. Fluids (resulting, for example, from the decomposition of phengite) probably facilitated melt generation. Peak temperatures during this stage of heating should have been at least 800 °C at P = 1.5 GPa, as inferred from petrological data for the eclogite boudins enclosed in the orthogneisses (Liati and Seidel 1996). However, even higher temperatures, on the order of at least 830 °C at 1.8 GPa; may have been reached (Fig. 9). An average pressure between 1.5 and 1.8 GPa (=1.65 GPa corresponding to ca 50 km depth) is assumed for the peak temperatures in this paper. Thus, at 40.0 ± 1.0 Ma, the rocks experienced the highest temperatures, on the order of 800 °C, when they were at depths of ca 50 km. The ca 42 Ma age obtained from the eclogite (42.2 ± 0.9 Ma) and orthogneiss (42.0 ± 1.1 Ma) zircons seems to be related to a time prior to leucosome formation (at 40.0 ± 1.0 Ma), when large amounts of fluids were also present (breakdown of paragonite; see above, section 7) and the rocks were at depths greater than ca 50 km, i.e., closer to the P-peak. Whether this was before or after the initiation of exhumation is uncertain because we do not know the precise P-peak conditions of the eclogite-facies stage. Nevertheless, it is evident that the age of 42 Ma should approximate the stage of the metamorphic cycle related to the P-peak.

All the SHRIMP data of this study were used to compile a P-T-$t_{(abs)}$ path (Fig. 9) for the evolution of the HP rocks of the upper tectonic unit of central Rhodope, based on the P-T-$t_{(rel)}$ path calculated on petrological grounds (Liati and Seidel 1996). As is shown in this figure, the shape of the prograde and retrograde trajectories are similar.

Geospeedometry

The P-T-$t_{(abs)}$ path of Fig. 9 provides a suitable basis for the calculation of rates of heating, cooling, burial, subduction and exhumation. In the absence of a precise determination of the P-T conditions for the formation of the 45.3 ± 0.9 Ma old prograde quartz vein, we can assume a temperature of 300 °C and a corresponding depth of ca 10 km. As already mentioned (section 7.1), PT conditions between 250 and 300 °C are reported for the first formation of such veins in several areas around the world (i.e., McNamara 1965). Although quartz veins of that type may form in a wider range of conditions, our assumption is based on the most likely scenario. As shown just below, even if the early deformed quartz vein formed at higher P and T, this does not lead to any considerable deviation in our calculations. Taking the 40.0 ± 1.0 Ma (age of the leucosome) for the T-peak (> 800 °C), we can calculate average heating rates as follows: 800 °C (T-peak) −300 °C (most likely T of formation of the early quartz vein) = 500 °C; 45.3 ± 0.9 Ma (age of the prograde quartz vein) −40.0 ± 1.0 Ma (age of the leucosome) = 5.3 ± 1.9 Ma. The resulting average heating rates are therefore 94 °C/Ma for the weighted mean age. Considering extreme error values, heating rates of 69 °C/Ma and 147 °C/Ma arise. It should be noted that since our errors are given at the 95% confidence level, it is rather unlikely that maximum errors apply and even less likely that lowermost and uppermost extreme age values apply simultaneously for both rock types considered in the calculations.

Assuming temperatures of quartz vein formation to have been 50 °C lower or higher (that is 250 or 350 instead of 300 °C), heating rates are shifted by ca 9 °C/Ma, which is negligible. It is clear therefore that uncertainty about the temperature of formation of the quartz vein hardly matters for the calculated heating rates.

Following the same procedure as described above for the heating rates, we calculated average values for burial rates (15 km/Ma), cooling rates (128 °C/Ma) and exhumation rates (7.7 km/Ma). The results are summarized in Table 3. The petrological data available establish only minimum P and T estimates. Thus, the above estimated rates are also minimum values.

Considering a subduction angle of 30°, subduction speeds of 30 km/Ma (or 30 mm/a) are calculated, which correspond to a spreading rate of 26.2 mm/a (0.1 GPa = 3 km in the calculations). Burial rates are lowered by 1.5 km/Ma if the formation of the quartz vein took place at higher P conditions, that is at 15 km instead of 10 km depth. The heating and burial rates, as well as the cooling and exhumation rates calculated here are only average rates, i.e., all these parameters may vary continuously along the P-T-t path.

The relatively high exhumation rates calculated for the Rhodope on the basis of the SHRIMP results are in line with petrological observations that (1) abundant symplectites are preserved in the overprinted eclogites, which requires fast cooling and exhumation rates, and that (2) intense prograde (growth) zoning of garnet in the kyanite eclogites is preserved (Liati and Seidel 1996). This indicates that the rocks did not stay long under high temperature conditions, which would cause homogenization of garnet.

To our knowledge, estimates of burial and heating rates reported in the literature are usually significantly lower than those deduced in the present study. However, rather high cooling and exhumation rates, comparable to our estimates, are reported for some metamorphic terranes. In the Spanish Betics, e.g., in the

Table 3 Calculation of heating rates (*HR*), cooling rates (*CR*), burial rates (*BR*) and exhumation rates (*ER*) for the tectono-metamorphic evolution of Rhodope, based on petrological and SHRIMP data

Rock type used	*T* of formation	ΔT	Age (Ma)	Difference in age ± extreme errors	Calculated average HR	Extreme HR values[a]
Calculation of heating rates (HR)						
Quartz vein	300 °C	500 °C	45.3 ± 0.9	5.3 ± 1.9	94 °C/Ma	69 °C/Ma
Leucosome	800 °C		40.0 ± 1.0			147 °C/Ma
Calculation of cooling rates (CR)					Calculated average CR	Extreme CR values[a]
Leucosome	800 °C	500 °C	40.0 ± 1.0	3.9 ± 1.2	128 °C/Ma	82 °C/Ma
Pegmatite	300 °C		36.1 ± 1.2			294 °C/Ma
Rock types used	Depth of formation	Depth difference	Age (Ma)	Difference in age ± extreme errors	Calculated average BR	Extreme BR values[a]
Calculation of burial rates (BR)						
Quartz vein	10 km	47 km	45.3 ± 0.9	3.1 ± 1.8	15 km/Ma	10 km/Ma
Eclogites	57 km		42.2 ± 0.9			36 km/Ma
Calculation of exhumation rates (ER)					Calculated average ER	Extreme ER values[a]
Eclogite	57 km	47 km	42.2 ± 0.9	6.1 ± 2.1	7.7 km/Ma	5.7 km/Ma
Pegmatite	10 km		36.1 ± 1.2			11.8 km/Ma

[a] Extreme HR, CR, BR and ER values are calculated by assuming the extreme error values to apply simultaneously for both rock types considered

Velez-Malaga-Torrox area, minimum cooling rates of 200 °C/Ma and minimum average "uplift rates" of 2.5–5 km/Ma are reported (Zeck et al. 1989), while for the same area Monié et al. (1994) conclude that cooling and exhumation rates were on the order of 100–350 °C/Ma and 3 km/Ma, respectively. Zeck et al. (1992) suggest that, for a major part of the Betic Cordileras, cooling rates were in the range of 150–350 °C/Ma and exhumation rates 5–10 km/Ma. For the Western Betics, Monié et al. (1994) suggest an exhumation rate of 10 km/Ma. For the south-east Tauern Window, Cliff et al. (1985) suggest that rates of exhumation varied with time and stage of the metamorphic evolution from >5 km/Ma to <1 km/Ma. Very high cooling and exhumation rates have also been reported for the UH*P* ultramafic/mafic rocks and their country rocks at Alpe Arami in the Central Swiss Alps (Gebauer 1996). Here, depending on the petrological data and omitting the hypothesis on an origin in the transition zone, the peridotites were exhumed from the mantle to the base of the crust with average rates of 12 km/Ma and a maximum rate of 32 km/Ma. In contrast to the exhumation rates, cooling rates reached maximum values of around 100 °C/Ma at crustal levels. Average exhumation and cooling rates for the UH*P*-terrane of Dora Maira (Western Alps) are 22 km/Ma and ca 90 °C/Ma (Gebauer et al. 1997), similar to values for eclogites from the upper Kaghan valley in the Himalaya of Pakistan (Spencer and Gebauer 1996). Thus, both average cooling and exhumation rates of >128 °C/Ma and >7.7 km/Ma, as derived for the Rhodope in this study, fit very well with the range of values deduced from recent geochronological data worldwide.

Geodynamic implications – conclusions

The Rhodope zone constitutes the largest, the highest grade and the highest pressure metamorphic part of the Alpine chain in Greece. A correlation of the metamorphic events between the Rhodope zone and the Attic–Cycladic Complex to the south reveals that the Rhodope was subducted at similar times as the Attic–Cycladic Complex, where Eocene ages are also reported for H*P* (eclogite-facies) metamorphism (e.g., 40–45 Ma; Altherr et al. 1979; Maluski et al. 1987; Wijbrans et al. 1990; Bröcker et al. 1993). The Cyclades and the central Rhodope may therefore be part of the same continental crust subducted northwards below the European plate. However, the 25 Ma age reported for the greenschist-facies metamorphic overprint in the Cyclades (e.g., Andriessen et al. 1979; Altherr et al. 1982) indicates that either the Cyclades were exhumed much more slowly than the Rhodope or that the radiometric 25 Ma age is due to reheating, possibly because of slab delamination (e.g., von Blanckenburg and Davies 1995).

The SHRIMP results presented in this paper, combined with previous petrological data, lead to the following conclusions:

1. Hercynian continental crust (probably containing oceanic remnants) formed at 294 ± 8 Ma and was subducted in the Eocene. The early stages of subduction (ca 300 °C, 0.3 GPa) occurred at 45.3 ± 0.9 Ma. Maximum depth was approached at 42.2 ± 0.9 Ma and maximum temperatures were reached at 40.0 ± 1.0 Ma. Late stages of the exhumation (ca 300 °C, 0.3 GPa) occurred at 36.1 ± 1.2 Ma.

2. The almost identical metamorphic age of the eclogites and country rock orthogneisses (42.2 ± 0.9 Ma and 42.0 ± 1.1 Ma, respectively) indicates that the eclogites were metamorphosed "in situ" together with the orthogneisses.

3. Calculated (average) rates of heating and burial during subduction (above ca 300 °C, 0.3 GPa) were > 94 °C/Ma and > 15 km/Ma (or 15 mm/a) and rates of cooling and exhumation (also above 300 °C, 0.3 GPa) were > 128 °C/Ma and > 7.7 km/Ma (or 7.7 mm/a).

4. Generally, fast exhumation of large masses of continental crust over ca 50 km in only about 6 Ma require new numerical modeling of heat and mass transfer, deformation and exhumation. This would give new insight into the mechanical behavior of the lithosphere.

The SHRIMP results of this study should not be extrapolated to the whole Rhodope zone. In east Rhodope, for instance, SHRIMP data on eclogites (Gebauer and Liati 1997 and unpublished data) indicate an age of ca 120 Ma for the gabbroic protolith and an age of ca 73 Ma for the H*P* metamorphism. These age data are in line with the presence of "Maastrichtian–Paleocene sediments discordantly overlying the crystalline basement" (Goranov and Athanasov 1992) in the area of Krumovgrad, in the Bulgarian part of east Rhodope, ca 20 km north of the eclogites dated by SHRIMP. This indicates that distinct geological units of the Rhodope zone were metamorphosed to high pressures at different times, favoring the former existence of different terranes. Moreover, the short time period between H*P* metamorphism and deposition of Maastrichtian-Paleocene sediments is an independent evidence for rapid exhumation also for east Rhodope. It is in very good agreement with the relatively high exhumation rates deduced in the present study for central Rhodope and suggested recently for many other orogens worldwide.

Acknowledgements We gratefully acknowledge the help of W. Compston, I.S. Williams and R. Wysoczanski at ANU (Canberra) and R.A. Stern at GSC (Ottawa) during various stages of SHRIMP data production and evaluation. We thank W. Wittwer for the tedious work involved in separating zircons. We also thank N. Mancktelow, ETH Zürich, whose corrections and suggestions helped to improve the text. Constructive reviews by R. Altherr, Heidelberg, and K. Mezger, Mainz, led to significant improvement of the manuscript. This work was supported by a grant of the Swiss National Science Foundation (20-42230.94).

References

Altherr R, Schliestedt M, Okrusch M, Seidel E, Kreuzer H, Harre W, Lenz H, Wendt I, Wagner GA (1979) Geochronology of high-pressure rocks on Sifnos (Cyclades, Greece). Contrib Mineral Petrol 70: 245–255

Altherr R, Kreuzer H, Wendt I, Lenz H, Wagner GA, Keller J, Harre W, Hohndorf (1982) A late Oligocene/early Miocene high temperature belt in the Attic–Cycladic crystalline complex (SE Pelagonian, Greece). Geol J b 23: 97–164

Andriessen PAM, Boelrijk NAIM, Hebeda EH, Priem HNA, Verdumen EATh, Verschure RH (1979) Dating the events of metamorphism and granitic magmatism in the Alpine orogene of Naxos (Cyclades, Greece). Contrib Mineral Petrol 69: 215–225

Arnaudov V, Amov B, Baldjieva M, Pavlova M (1990) Tertiary migmatic pegmatites in Central Rhodope crystalline complex: uranium-lead zircon dating. Geol Balc 20(6): 25–32

Borsi S, Ferrara G, Mercier J (1965) Détérmination de l'age des séries métamorphiques du Massif Serbomacédonien au Nord-Est de Thessalonique (Grèce) par les méthodes Rb/Sr et K/Ar. Ann Soc Geol Nord 84: 223–225

Bröcker M, Kreuzer H, Matthews A, Okrusch M (1993) $^{40}Ar/^{39}Ar$ and oxygen isotope studies of polymetamorphism from Tinos island, Cycladic blueschist belt, Greece. J Metamorphic Geol 11: 223–240

Burchfiel BC (1980) Eastern European Alpine system and the Carpathian orocline as an example of collision tectonics. Tectonophysics 63: 31–61

Burg JP, Godfriaux I, Ricou LE (1995) Extension of the Mesozoic Rhodope thrust units in the Vertiskos–Kerdyllion Massifs (Northern Greece). CR Acad Sci Paris t.320, série II a: 889–896

Burg JP, Ricou LE, Ivanov Z, Godfriaux I, Dimov D, Klain L (1996) Syn-metamorphic nappe complex in the Rhodope Massif: structure and kinematics. Terra Nova 8: 6–15

Cliff RA, Droop GTR, Rex DC (1985) Alpine metamorphism in the south-east Tauern Window, Austria. 2. Rates of heating, cooling and uplift. J Metamorphic Geol 3: 403–415

Cumming GL, Richards GR (1975) Ore lead isotope ratios in a continuously changing Earth. Earth Planet Sci Lett 28(2): 155–171

Dinter DA, Macfarlane A, Hames W, Isachsen C, Bowring S, Royden L (1995) U-Pb and 40Ar/39Ar geochronology of the Symvolon granodiorite: Implications for the thermal and structural evolution of the Rhodope metamorphic core complex, northeastern Greece. Tectonics 14: 886–908

Dinter DA, Royden L (1993) Late Cenozoic extension in northeastern Greece: Strymon valley detachment system and Rhodope metamorphic core complex. Geology 21: 45–48

Gebauer D (1996) A *P-T-t* path for (ultra?-) high-pressure ultramafic/mafic rock associations and their felsic country rocks based on SHRIMP dating of magmatic and metamorphic zircon domains: example: Alpe Arami (Central Swiss Alps). In: Basu A, Hart S (eds) Earth processes: reading the isotopic code. (Spec AGU-Monogr dedicated to Profs, Tilton and Tatsumoto): Geophys Monogr Ser 95, pp 307–329

Gebauer D, Liati A (1997) Geochronological evidence for Mesozoic rifting and oceanization followed by Eocene subduction in the Rhodope Complex (Northern Greece) (abstract). Terra Nova 9, Abstr Suppl 1: 10

Gebauer D, Schertl HP, Brix M, Schreyer W (1997) 35 Ma old ultrahigh-pressure metamorphism and evidence for very rapid exhumation in the Dora Maira Massif, Western Alps. Lithos 41: 5–24

Goranov A, Athanasov G (1992) Lithostratigraphy and formation conditions of Maastrichtian–Paleocene deposits in Krumovgrad district. Geol Balc 22 (3): 71–82

Graham CM, Powell R (1984) A garnet-hornblende geothermometer: calibration, testing and application to the Pelona Schist, southern California. J Metamorphic Geol 2: 13–21

Harre W, Kockel F, Kreuzer H, Lenz H, Müller P, Walter HW (1968) ber Rejuvenationen im Serbo-Mazedonischen Massif (Deutung radiometrischer Altersbestimmungen). 23rd Int Geol Congr Prague 6: 223–236

Heinrich CA (1982) Kyanite–eclogite to amphibolite facies evolution of hydrous mafic and pelitic rocks, Adula Nappe, central Alps. Contrib Mineral Petrol 81: 30–38

Jamtveit B, Yardley WD (1997) Fluid flow and transport in rocks: an overview. In: Jamtveit B, Yardley WD (eds): Fluid flow and transport in rocks: mechanisms and effects. Chapman and Hall, London pp 1–14

Jones C, Tarney J, Barreiro B (1994) The make-up and melting of a subduction-accretion complex: generation of S- and I-type granitoids (abstract). In: Abstr 8th Int Conf Geochronal Cosmochronal Isot Geol, Berkeley, CA, p 160

Kelley SP, Arnaud NO, Okay AI (1994) Anomalously old Ar-Ar ages in high pressure metamorphic terrains. Mineral Mag 58A: 468–469

Kockel F, Walther HW (1965) Die Strymon Linie als Grenze zwischen Serbo-Mazedonischem und Rila-Rhodope Massiv in Ost Mazedonien. Geol J b 83: 575–602

Kohn MJ, Spear FS (1989) Empirical calibration of geobarometers for the assemblage garnet + hornblende + plagioclase + quartz. Am Mineral 74: 77–84

Liati A (1986) Regional metamorphism and overprinting contact metamorphism of the Rhodope zone, near Xanthi, N. Greece: petrology, geochemistry, geochronology. Diss, Tech Univ Braunschweig, Germany

Liati A, Kreuzer H (1990) K-Ar dating of metamorphic and magmatic rocks from the Xanthi and Drama areas, Greek part of the Rhodope zone (abstract). Eur J Mineral 2: 161

Liati A, Seidel E (1996) Metamorphic evolution and geochemistry of kyanite eclogites in central Rhodope, northern Greece. Contrib Mineral Petrol 123: 293–307

Maluski H, Bonneau M, Kienast J (1987) Dating the metamorphic events in the Cycladic area: $^{40}Ar/^{39}Ar$ data from the island of Syros (Greece). Bull Soc Geol Fr 5: 833–842

Manning CE (1996) Effect of sediments on aqueous silica transport in subduction zones. Am Geophys Union Geophys Monogr 96: 277–284

Mc Laren AC, Fitzgerald JD, Williams IS (1994) The microstructure of zircon and its influence on the age determination from Pb/U isotopic ratios measured by ion microprobe. Geochim Cosmochim Acta 58: 607–610

McNamara M (1965) The lower greenschist facies in the Scottish Highlands. Geol Foerh Stockholm Foeren 87: 247–389

Monié P, Torres-Roldan RL, Garcia-Casco A (1994) Cooling and exhumation of the Western Betic Cordilleras, $^{40}Ar/^{39}Ar$ thermochronological constraints on a collapsed terrane. Tectonophysics 238: 353–379

Mposkos E (1989) High-pressure metamorphism in gneisses and pelitic schists in East Rhodope zone (N. Greece). Mineral Petrol 41: 337–351

Papadopoulos C, Kilias A (1985) Altersbeziehumgen zwischen Metamorphose und Deformation im zentralen Teil des Serbomazedonischen Massivs (Vertiskos Gebirge, Nord-Griechenland). Geol Rundsch 74: 77–85

Papanikolaou D, Panagopoulos G (1981) On the structural style of Southern Rhodope (Greece). Geol Balc 11(3): 13–22

Peytcheva I, von Quadt A (1995) U-Pb zircon dating of metagranites from Byala Reka region in the East Rhodopes, Bulgaria. Geol Soc Greece Spec Publ 4(2): 637–642

Spencer D, Gebauer D (1996) SHRIMP evidence for a Permian protolith age and a 44 MA metamorphic age for the Himalayan eclogites (Upper Kaghan, Pakistan): implications for the subduction of Tethys and the subdivision terminology of the NW Himalaya (abstract). 11th Himalayan-Karakoram-Tibet Workshop, Flagstaff, Arizona, USA, Abstr Vol, pp 147–150

Vavra F, Gebauer D, Schmid R, Compston W (1996) Multiple zircon growth during polyphase latest Carboniferous to Triassic metamorphism in granulites of the Ivrea Zone (Southern Alps): an ion microprobe (SHRIMP) study. Contrib Mineral Petrol 122: 337–358

von Blanckenburg F, Davies JH (1995) Slab breakoff: a model for syncollisional magmatism and tectonics in the Alps. Tectonics 14: 120–131

Wawrzenitz N (1997) Mikrostrukturell unterstützte Datierung von Deformationsinkrementen in Myloniten: Dauer der Exhumierung und Aufdomung des metamorphen Kernkomplexes der Insel Thassos (Süd-Rhodope, Nordgriechenland). Diss, Univ Erlangen, Nürnberg

Wijbrans JR, Schliestedt M, York D (1990) Single grain argon laser probe dating of phengites from the blueschist to greenschist transition on Sifnos (Cyclades, Greece). Contrib Mineral Petrol 104: 582–593

Williams IS, Buick S, Cartwright I (1996) An extended episode of early Mesoproterozoic metamorphic fluid flow in the Reynolds Range, central Australia. J Metamorphic Geol 14: 29–47

Yardley WD (1997) The evolution of fluids through the metamorphic cycle. In: Jamtveit B, Yardley WD (eds) Fluid flow and transport in rocks: mechanisms and effects, Chapman and Hall, London pp 99–121

Zeck HP, Albat F, Hansen BT, Torres-Roldan RL, Garcia-Casco A, Martin-Algarra A (1989) A 21 ± 2 Ma age for the termination of the ductile Alpine deformation in the internal zone of the Betic Cordilleras, South Spain. Tectonophysics 169: 215–220

Zeck HP, Monié P, Villa IM, Hansen BT (1992) High rates of cooling and uplift in the Betic Cordilleras, S. Spain Alpine lithospheric slab detachment, mantle diapirism and extensional tectonics. Geology 20: 79–82